

Multiphoton interaction of a qutrit with single-mode quantized field in the ultrastrong and deep strong coupling regimes

H.K. Avetissian¹, A.K. Avetissian¹, G.F. Mkrtchian¹, and O.V. Kibis²

¹ *Centre of Strong Fields Physics, Yerevan State University, 1 A. Manukian, Yerevan 0025, Armenia and*

² *Department of Applied and Theoretical Physics, Novosibirsk State Technical University, Karl Marx Avenue 20, 630073 Novosibirsk, Russia*

We consider multiphoton dynamics of a quantum system composed of a three-state atom (a qutrit) and a single-mode photonic field in the ultrastrong and deep strong coupling regimes, when the coupling strength is comparable to or larger than the oscillator energy scale. We assume a qutrit to be in a polar- Λ configuration in which two lower levels have mean dipole moments. Direct multiphoton resonant transitions revealing generalized Rabi oscillations, collapse, and revivals in atomic excitation probabilities for the ultrastrong couplings are studied. In the deep strong coupling regime particular emphasis is placed on the ground state of considering system which exhibits strictly nonclassical properties.

PACS numbers: 42.50.Hz, 42.50.Dv, 85.25.Hv, 42.50.Pq

I. INTRODUCTION

Quantum dynamic interactions involving a quantum system with a few energy levels and one or more near-resonant modes of the quantized photonic field have been extensively studied by means of various models. Such combined systems are shown to exhibit interesting non-classical effects, such as the collapse and revival of the Rabi oscillations of the atomic inversion, antibunched light, squeezing, and etc. [1, 2]. Among these models the so called Jaynes-Cummings (JC) model [3], which describes a two-level system coupled to a quantum harmonic oscillator (e.g., a single radiation mode) has many applications in various branches of contemporary physics ranging from quantum optics/informatics [4–6] to condensed matter physics [7–9].

With the three-state quantum system, depending on the levels' linkages, one can enrich the conventional JC model including new effects connected with the quantum interference effects. With respect to simple two-level systems, in the three-level system an extra level can be used for effective manipulation of remaining two levels or so called qubits. Otherwise, three-state quantum system as a whole can be used as a unit for storing quantum information. In the latter case as a unit of quantum information stands for qutrit, which has several specific features providing significant improvements over qubits for several quantum protocols [10]. The various cases of three-state atoms coupled to a quantized field have been treated by many authors (see [1] and references therein). The considered linkages are the ladder (Ξ), the vee (V), and the lambda (Λ). As has been shown in Refs. [11, 12], there is another three-state configuration -one can refer it as a Γ configuration, where multiphoton transitions in the quantum dynamics of the system subjected to a classical radiation field are very effective compared to the

Ξ , V , and Λ configurations. In this case lower level is coupled to an upper level which in turn is coupled to an adjacent level. If the energies of excited states in Γ configuration are enough close to each other then by the unitary transformation the problem can be reduced to the polar- V configuration, i.e. with permanent dipole moments in the excited stationary states. In this context as a known example one can mention the hydrogen atom in spheric and parabolic [13] coordinates. The inverse with respect to the Γ configuration is the L configuration, which is unitary equivalent to the polar- Λ configuration (see below). Thus, it is of interest to study the interaction of L -type (or Γ -type) atom with single-mode quantized radiation field, where new multiphoton effects are expected. Thanks to recent achievements in Cavity/Circuit Quantum Electrodynamics (QED) [14] one can achieve interaction-dominated regimes in which multiphoton effects are expected. The key parameter to characterize Cavity/Circuit Quantum Electrodynamics (QED) setups is the vacuum Rabi frequency, which is the strength of the coupling between the light and matter. Depending on the magnitude of the vacuum Rabi frequency Cavity/Circuit QED can be divided into four coupling regimes: weak, strong, ultrastrong, and deep strong. For the weak coupling, the atom-photon interaction rate is smaller than the atomic and cavity field decay rates. In this case one can manipulate by the spontaneous emission rate compared with its vacuum level by tuning discrete cavity modes [15]. In the strong coupling regime, when the emitter-photon interaction becomes larger than the combined decay rate, instead of the irreversible spontaneous emission process coherent periodic energy exchange between the emitter and the photon field in the form of Rabi oscillations takes place [16]. In the ultrastrong coupling regime, the emitter-photon coupling strength is comparable to appreciable fractions of the oscillator frequency [14, 17]. In this regime new nonlinear [18] and multiphoton [19] phenomena are visible that are not present in the weak or strong coupling regimes. If the emitter-photon coupling strength is increased even further it becomes

larger than the oscillator frequency. This regime, usually referred to as deep strong coupling regime, opens up new possibilities for matter–photon manipulations in the quantum level [20]. The main candidate for achieving deep strong coupling regime is the circuit QED setups [8] where one can realize artificial atoms with desired configuration [21, 22]. The main advantage of these atoms over natural ones is the additional control associated with the tunability of almost all parameters. In particular, one can realize three-state Δ -atom [21], opening possibilities for many quantum optics phenomena with superconducting circuits.

In the present paper we consider a quantum system composed of a three-level artificial atom (qutrit) and a single-mode photonic field, i.e. harmonic oscillator, in the ultrastrong and deep strong coupling regimes. We assume a qutrit to be in a polar- Λ configuration in which two lower levels have mean dipole moments. We consider direct multiphoton resonant transitions for the ultrastrong coupling regime. In the deep strong coupling regime particular emphasis is placed on the ground state of the system. The latter exhibits strictly nonclassical properties, which ensures controllable implementation of qutrit-oscillator entangled states.

The paper is organized as follows. In Sec. II the model Hamiltonian is introduced and diagonalized in the scope of a resonant approximation. In Sec. III we consider temporal quantum dynamics of considered system and present corresponding numerical simulations. In Sec. IV we present results of numerical calculations that demonstrate the properties of the system in the deep strong coupling regime. In particular, we consider quantum features of the ground state. Finally, conclusions are given in Sec. V.

II. BASIC HAMILTONIAN AND RESONANT APPROXIMATION

Let us consider a three-state quantum system or so called qutrit interacting with the single-mode radiation field of frequency ω . Schematic illustration of the system under consideration is shown in Fig. 1. We assume a qutrit to be in a polar- Λ configuration in which two lower levels $|g_1\rangle$ and $|g_2\rangle$ with mean dipole moments are coupled to a single upper level $|e\rangle$. Other possible three-level scheme is shown in the lower part of Fig. 1 and one can refer it as a L configuration. In this case upper level is coupled to a lower level which in turn is coupled to an adjacent level. For the L configuration the mean dipole moment is zero for a stationary states. The polar- Λ configuration is unitary equivalent to a L configuration. A more in-depth discussion of this point can be found in Appendix A. The mentioned qutrit configuration can be realized for example in the symmetric double well potential. The latter is a frequently appearing structure in the solid-state semiconductor or superconductor systems [23]. In particular, the effective potential

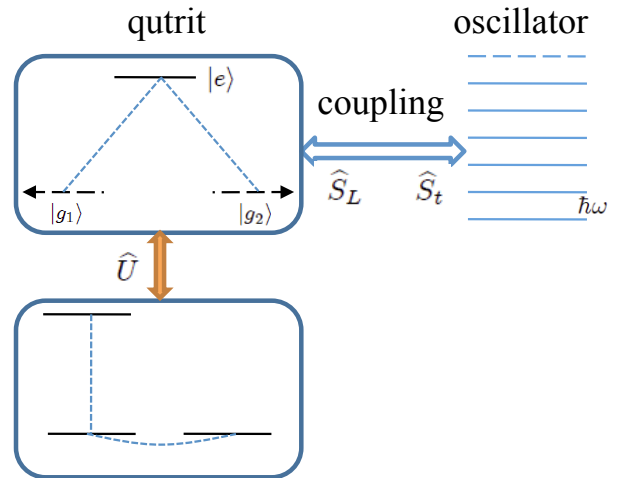


FIG. 1: Schematic illustration of the system under consideration. A qutrit in polar- Λ configuration is coupled to a quantized single-mode field, represented as a harmonic oscillator with characteristic frequency ω . Here two lower levels $|g_1\rangle$ and $|g_2\rangle$ with mean dipole moments are coupled to a single upper level $|e\rangle$. The considered configuration is unitary equivalent to a L configuration shown in the lower part of diagram. In this case upper level is coupled to a lower level which in turn is coupled to an adjacent level.

landscape is reduced to a double-well potential for superconducting quantum interference device loop [24] and three-Josephson junction loop [25].

Here we assume coupling to a bosonic field with the transition selection rules equivalent the ones for the electric-dipole transitions in usual atoms. For the artificial atom based on the superconducting quantum circuit the eigenstates involve macroscopic number of electrons. However, as was shown in Refs. [21, 22] the optical selection rules of the microwave-assisted transitions in a flux qubit superconducting quantum circuit are the same as the ones for the electric-dipole transitions in usual atoms when effective potential landscape is reduced to a symmetric double-well potential.

Thus, assuming the basis

$$|g_1\rangle = \begin{pmatrix} 1 \\ 0 \\ 0 \end{pmatrix}, |g_2\rangle = \begin{pmatrix} 0 \\ 1 \\ 0 \end{pmatrix}, |e\rangle = \begin{pmatrix} 0 \\ 0 \\ 1 \end{pmatrix}, \quad (1)$$

the Hamiltonian for the polar- Λ system coupled to a bosonic field will be presented in the form:

$$\begin{aligned} \hat{H} = & \hbar\omega \left(\hat{a}^\dagger \hat{a} + \frac{1}{2} \right) + \hat{H}_\Lambda \\ & + \hbar \left(\mu \hat{S}_L + \lambda \hat{S}_t \right) (\hat{a}^\dagger + \hat{a}). \end{aligned} \quad (2)$$

The first term in Eq. (2) corresponds to the free harmonic oscillator of frequency ω (single-mode radiation

field). The second term:

$$\hat{H}_\Lambda = \begin{pmatrix} \varepsilon_g & \Delta & 0 \\ \Delta & \varepsilon_g & 0 \\ 0 & 0 & \varepsilon_e \end{pmatrix} \quad (3)$$

corresponds to the three-level system. Here nondiagonal elements (Δ) describe transitions between lower laying states (tunnel transition). The final term in Eq. (2) gives the interaction between the single-mode radiation field and qutrit. Creation and annihilation operators, \hat{a}^+ and \hat{a} , satisfy the bosonic commutation rules. The operator

$$\hat{S}_L = -|g_1\rangle\langle g_1| + |g_2\rangle\langle g_2| = \begin{pmatrix} -1 & 0 & 0 \\ 0 & 1 & 0 \\ 0 & 0 & 0 \end{pmatrix} \quad (4)$$

is the result of the mean dipole moments in the states of indefinite parity. The operator

$$\hat{S}_t = |g_1\rangle\langle e| - |g_2\rangle\langle e| + \text{h.c.} = \begin{pmatrix} 0 & 0 & 1 \\ 0 & 0 & -1 \\ 1 & -1 & 0 \end{pmatrix} \quad (5)$$

describes transition between excited and lower laying states. At $\mu = 0$ we have the usual Hamiltonian for Λ model. At $\lambda = 0$ the excited state is decoupled and after unitary transformation (A4) one will obtain usual Hamiltonian for JC model (including also counter-rotating terms) with coupling $\hbar\mu$ and atomic energy 2Δ . Thus, to emphasize three-state structure in this paper we will consider the case $|\Delta| \ll \hbar\omega < \varepsilon_e - \varepsilon_g$.

At first, we will diagonalize the Hamiltonian (2) for the moderately strong couplings, which is straightforward in the resonant case. For the case $\Delta = 0$, the Hamiltonian (2) can be rewritten in the form:

$$\hat{H} = \hat{H}_0 + \hat{V}, \quad (6)$$

where

$$\hat{H}_0 = \hat{H}_{os} \otimes \hat{P}_e + \hat{H}_- \otimes \hat{P}_{g_1} + \hat{H}_+ \otimes \hat{P}_{g_2} \quad (7)$$

represents three non-coupled oscillators. Here $\hat{P}_{g_1} = |g_1\rangle\langle g_1|$, $\hat{P}_{g_2} = |g_2\rangle\langle g_2|$, and $\hat{P}_e = |e\rangle\langle e|$ are projection operators. The excited state is associated to normal oscillator with the Hamiltonian

$$\hat{H}_{os} = \hbar\omega \left(\hat{a}^+ \hat{a} + \frac{1}{2} \right) + \varepsilon_e, \quad (8)$$

while two others are associated to position-displaced oscillators

$$\hat{H}_- = \hbar\omega \left(\hat{a}^+ \hat{a} + \frac{1}{2} \right) + \varepsilon_g - \hbar\mu (\hat{a}^+ + \hat{a}), \quad (9)$$

$$\hat{H}_+ = \hbar\omega \left(\hat{a}^+ \hat{a} + \frac{1}{2} \right) + \varepsilon_g + \hbar\mu (\hat{a}^+ + \hat{a}). \quad (10)$$

The interaction part

$$\hat{V} = \hbar\lambda \hat{S}_t (\hat{a}^+ + \hat{a}) \quad (11)$$

in Eq. (6) couples \hat{H}_{os} with \hat{H}_- and \hat{H}_+ . Hamiltonians (8), (9), and (10) admit exact diagonalization. It is easy to see that the corresponding eigenstates are

$$\begin{aligned} |e, N^{(os)}\rangle &\equiv |e\rangle \otimes |N\rangle, \\ |g_1, N^{(-)}\rangle &\equiv |g_1\rangle \otimes e^{(\mu/\omega)(\hat{a}^\dagger - \hat{a})} |N\rangle, \\ |g_2, N^{(+)}\rangle &\equiv |g_2\rangle \otimes e^{-(\mu/\omega)(\hat{a}^\dagger - \hat{a})} |N\rangle, \end{aligned} \quad (12)$$

with energies

$$\begin{aligned} E_{eN} &= \varepsilon_e + \hbar\omega(N + \frac{1}{2}), \\ E_{g_1N} &= E_{g_2N} = \varepsilon_g + \hbar\omega(N + \frac{1}{2}) - \hbar\frac{\mu^2}{\omega}. \end{aligned} \quad (13)$$

Here $D(\alpha) = e^{\alpha(\hat{a}^\dagger - \hat{a})}$ is the displacement operator and quantum number $N = 0, 1, \dots$. The states $|N^{(+)}\rangle$, $|N^{(-)}\rangle$ are position-displaced Fock states:

$$\begin{aligned} |N^{(+)}\rangle &= e^{-(\mu/\omega)(\hat{a}^\dagger - \hat{a})} |N\rangle = \sum_M I_{N,M} \left(\frac{\mu^2}{\omega^2} \right) |M\rangle, \\ |N^{(-)}\rangle &= e^{(\mu/\omega)(\hat{a}^\dagger - \hat{a})} |N\rangle = \sum_M I_{M,N} \left(\frac{\mu^2}{\omega^2} \right) |M\rangle, \end{aligned} \quad (14)$$

where $I_{N,M}(\alpha)$ is the Laguerre function and defined via generalized Laguerre polynomials $L_n^l(\alpha)$ as follows:

$$\begin{aligned} I_{s,s'}(\alpha) &= \sqrt{\frac{s'!}{s!}} e^{-\frac{\alpha}{2}} \alpha^{\frac{s-s'}{2}} L_{s'-s'}^{s-s'}(\alpha) = (-1)^{s-s'} I_{s',s}(\alpha), \\ L_n^l(\alpha) &= \frac{1}{n!} e^\alpha \alpha^{-l} \frac{d^n}{d\alpha^n} (e^{-\alpha} \alpha^{n+l}). \end{aligned} \quad (15)$$

Particularly, $|0^{(+)}\rangle$ and $|0^{(-)}\rangle$ are the Glauber or coherent states with mean number of photons μ^2/ω^2 . Thus, we have three ladders, two of them are crossed, and one ladder shifted by the energy:

$$\hbar\omega_{eg} = \hbar(\omega_0 + \mu^2/\omega), \quad (16)$$

where $\omega_0 = (\varepsilon_e - \varepsilon_g)/\hbar$. The coupling term (11) $\hat{V} \sim \hat{S}_t$ induces transitions between these manifolds. At the resonance:

$$\omega_{eg} - \omega n = \delta_n; |\delta_n| \ll \omega \quad (17)$$

with $n = 1, 2, \dots$ the equidistant ladders are crossed: $E_{eN} \simeq E_{g_1N+n} = E_{g_2N+n}$, and the energy levels starting from the ground state of upper harmonic oscillators are nearly threefold degenerated. The coupling (11) removes this degeneracy, leading to "qutrit-photon" entangled states. The splitting of levels is defined by the vacuum multiphoton Rabi frequency. In this case we should

apply secular perturbation theory [13]. Taking into account that

$$\langle g_1, N^{(-)} | \hat{V} | e, N - n \rangle = (-1)^n \langle g_2, N^{(+)} | \hat{V} | e, N - n \rangle,$$

and searching for the solution in the form

$$\begin{aligned} |\alpha, N\rangle &= C_{g_1}^{(\alpha)} |g_1, N^{(-)}\rangle + C_{g_2}^{(\alpha)} |g_2, N^{(+)}\rangle \\ &+ C_e^{(\alpha)} |e, N - n\rangle, \end{aligned} \quad (18)$$

we get eigenenergies

$$E_{1,N} = \varepsilon_g + \hbar\omega(N + \frac{1}{2}) - \hbar\frac{\mu^2}{\omega}, \quad (19)$$

$$E_{2,N} = E_{1,N} + \sqrt{2} |V_N(n)|, \quad (20)$$

$$E_{3,N} = E_{1,N} - \sqrt{2} |V_N(n)|, \quad (21)$$

and corresponding eigenstates

$$|1, N\rangle = \frac{1}{\sqrt{2}} \left(|g_1, N^{(-)}\rangle + (-1)^{n+1} |g_2, N^{(+)}\rangle \right), \quad (22)$$

$$\begin{aligned} |2, N\rangle &= \frac{1}{2} |g_1, N^{(-)}\rangle + (-1)^n \frac{1}{2} |g_2, N^{(+)}\rangle \\ &+ \frac{e^{-i\varphi_{V_N}}}{\sqrt{2}} |e, N - n\rangle, \end{aligned} \quad (23)$$

$$\begin{aligned} |3, N\rangle &= \frac{1}{2} |g_1, N^{(-)}\rangle + (-1)^n \frac{1}{2} |g_2, N^{(+)}\rangle \\ &- \frac{e^{-i\varphi_{V_N}}}{\sqrt{2}} |e, N - n\rangle. \end{aligned} \quad (24)$$

In Eqs. (20)-(24) the transition matrix element is:

$$\begin{aligned} V_N(n) &\equiv \langle g_1, N^{(-)} | \hat{V} | e, N - n \rangle \\ &= \hbar\lambda\sqrt{N-n} I_{N-n-1,N} \left(\frac{\mu^2}{\omega^2} \right) \\ &+ \hbar\lambda\sqrt{N-n+1} I_{N-n+1,N} \left(\frac{\mu^2}{\omega^2} \right), \end{aligned} \quad (25)$$

and $\varphi_{V_N} = \arg[V_N(n)]$. Thus, starting from the level $N = n$ we have qutrit-photon entangled states (23) and (24), while for $N = 0, 1, \dots, n-1$ we have twofold degenerated eigenenergies $E_{1,N}$ with states $|g_1, N^{(-)}\rangle$ and $|g_2, N^{(+)}\rangle$. At the $\mu = 0$ similar to the conventional JC model there is a selection rule: $V_N(n) \neq 0$ only for $n = \pm 1$. In this case only one photon Rabi oscillations takes place. In our model with $\mu \neq 0$ there are transition with arbitrary n giving rise to multiphoton coherent transitions. The solutions (22)-(24) are valid at near multiphoton resonance $\omega_{eg} \simeq n\omega$ and weak coupling:

$$|V_N(n)| \ll \hbar\omega. \quad (26)$$

III. MULTIPHOTON RABI OSCILLATIONS IN THE ULTRA-STRONG COUPLING REGIME

In this section, we consider temporal evolution of the qutrit-photon field system. This is of particular interest for applications in quantum information processing. Here we also present numerical solutions of the time-dependent Schrödinger equation with the full Hamiltonian (2).

We first proceed to consider the quantum dynamics of the coupled qutrit-photon field starting from an initial state, which is not an eigenstate of the Hamiltonian (2). Assuming arbitrary initial state $|\Psi_0\rangle$ of a system, then the state vector for times $t > 0$ is just given by the expansion over the basis obtained above:

$$\begin{aligned} |\Psi(t)\rangle &= \sum_{N=0}^{n-1} \langle g_1, N^{(-)} | \Psi_0 \rangle e^{-\frac{i}{\hbar} E_{g_1, N} t} |g_1, N^{(-)}\rangle \\ &+ \sum_{N=0}^{n-1} \langle g_2, N^{(+)} | \Psi_0 \rangle e^{-\frac{i}{\hbar} E_{g_2, N} t} |g_2, N^{(+)}\rangle \\ &+ \sum_{\alpha=1}^3 \sum_{N=n}^{\infty} \langle \alpha, N | \Psi_0 \rangle e^{-\frac{i}{\hbar} E_{\alpha, N} t} |\alpha, N\rangle. \end{aligned} \quad (27)$$

For concreteness we will consider two common initial conditions for photonic field: the Fock state and the coherent state. We will calculate the time dependence of the three-level system population inversion

$$W_n(t) = \langle \Psi(t) | \hat{\Sigma}_z | \Psi(t) \rangle \quad (28)$$

at the exact n -photon resonance (17), where

$$\hat{\Sigma}_z = \begin{pmatrix} -1 & 0 & 0 \\ 0 & -1 & 0 \\ 0 & 0 & 1 \end{pmatrix}. \quad (29)$$

For the field in the vacuum state and two level system in the excited state $|\Psi_0\rangle = |e, 0\rangle$, from Eqs. (22)-(24), and (27) we have:

$$|\Psi(t)\rangle = \frac{e^{i\varphi_{V_n}}}{\sqrt{2}} e^{-\frac{i}{\hbar} E_{2,n} t} \left(|2, n\rangle - e^{i\Omega_n(n)t} |3, n\rangle \right), \quad (30)$$

where

$$\Omega_N(n) = \frac{2\sqrt{2} |V_N(n)|}{\hbar} \quad (31)$$

is the multiphoton vacuum Rabi frequency. From Eqs. (28)-(30) for the population inversion we obtain

$$W_n(t) = \cos(\Omega_n(n)t), \quad (32)$$

which corresponds to Rabi oscillations with periodic exchange of n photons between the qutrit and the radiation field.

Then we turn to the case in which a qutrit begins in the excited state, with a photonic field prepared in a coherent state with a mean photon number \bar{N} :

$$|\Psi_0\rangle = |e\rangle \otimes e^{\sqrt{\bar{N}}(\hat{a}^\dagger - \hat{a})}|0\rangle. \quad (33)$$

Taking into account Eqs. (27) and (33) for the wave function we obtain

$$|\Psi(t)\rangle = \sum_{N=n}^{\infty} \frac{e^{i\varphi_{V_N}}}{\sqrt{2}} I_{N-n,0}(\bar{N}) \left[e^{-\frac{i}{\hbar} E_{2,N} t} |2, N\rangle - e^{-\frac{i}{\hbar} E_{3,N} t} |3, N\rangle \right], \quad (34)$$

which in turn for population inversion (28) gives:

$$W_n(t) = \sum_{N=0}^{\infty} \frac{e^{-\bar{N}}}{N!} \bar{N}^N \cos[\Omega_{N+n}(n)t]. \quad (35)$$

In this case we have superposition of Rabi oscillations with the amplitudes given by the Poissonian distribution $P_N = e^{-\bar{N}} \bar{N}^N / N!$. As a consequence, we have collapse and revival phenomena of the multiphoton Rabi oscillations. There are dominant frequencies in Eq. (35) as a result of the spread of probabilities about \bar{N} for a photon numbers in the range $\bar{N} \pm \sqrt{\bar{N}}$. When these terms are oscillating out of phase with each other in the sum (35), it is expected cancellation of these terms, i.e. collapse of Rabi oscillations. Hence, for large photon numbers $\bar{N} \gg \sqrt{\bar{N}}$ the collapse time may be estimated as

$$t_c^{(n)} \simeq \frac{\pi}{2\sqrt{\bar{N}}} \left(\frac{\partial \Omega_N(n)}{\partial N} \right)^{-1}. \quad (36)$$

Taking into account Eq. (25), it follows that in contrast to conventional JC model the collapse time (36) strongly depends on the mean photon number. Now let us consider numerical solutions of the time dependent Schrödinger equation with the full Hamiltonian (2) in the Fock basis:

$$|\Psi(t)\rangle = \sum_{\sigma=g_1, g_2, e} \sum_{N=0}^{N_{\max}} C_{\sigma, N}(t) |\sigma\rangle \otimes |N\rangle. \quad (37)$$

The set of equations for the probability amplitudes $C_{\sigma, N}(t)$ has been solved using a standard fourth-order Runge-Kutta algorithm [26], considering up to $N_{\max} = 200$ excitations. To show periodic multiphoton exchange between the qutrit and the radiation field, we have calculated the population inversion (28) and the photon number probability:

$$P_N(t) = \sum_{\sigma=g_1, g_2, e} \langle \sigma, N | \Psi(t) \rangle \langle \Psi(t) | \sigma, N \rangle. \quad (38)$$

In Figs. (2) and (3) the photon number probability $P_N(t)$ as a function of time is shown for the two and

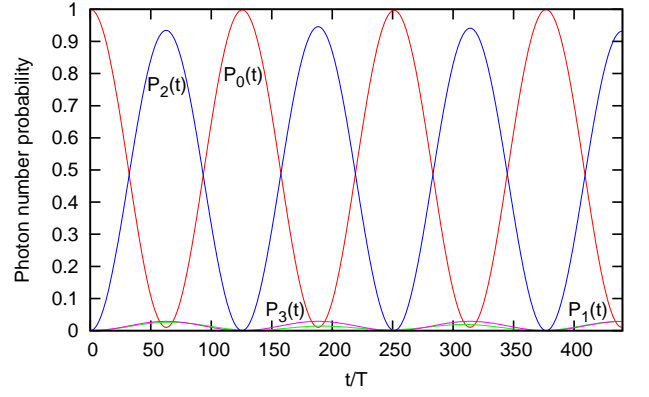


FIG. 2: (Color online) Photon number probability $P_N(t)$ as a function of scaled time at the two-photon resonance ($2\omega = \omega_{eg}$). $\lambda/\omega = 0.02$, $\mu/\omega = 0.1$.

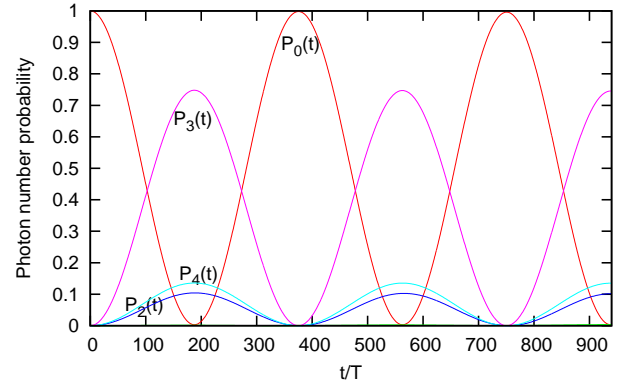


FIG. 3: (Color online) Photon number probability $P_N(t)$ as a function of scaled time at the three-photon resonance ($n = 3$). $\lambda/\omega = 0.02$, $\mu/\omega = 0.2$.

three photon resonances. For an initial state we assume qutrit in the excited state and the field in vacuum state - $|e\rangle \otimes |0\rangle$. The Schrödinger equation with the full Hamiltonian (2) was numerically solved with the tunneling parameter $\Delta = 0$. As is seen from these figures, due to the mean dipole moment, multiphoton Fock states are excited. Figure 4 displays collapse and revival of the multiphoton Rabi oscillations. Here the qutrit population inversion is shown with the field initially in a coherent state at two-, three-, and four-photon resonances for different mean photon numbers.

The consequence of collapse and revival of the multiphoton Rabi oscillations on the statistical properties of the photons shown in Fig. (5). For this propose we have calculated the Mandel's Q -factor defined as [4]:

$$Q = \frac{\overline{N^2} - \bar{N}^2 - \bar{N}}{\bar{N}}. \quad (39)$$

When $-1 \leq Q < 0$ ($Q > 0$), the statistics is sub-Poissonian (super-Poissonian) and $Q = 0$ shows the Poissonian statistics, which takes place for coherent state. As

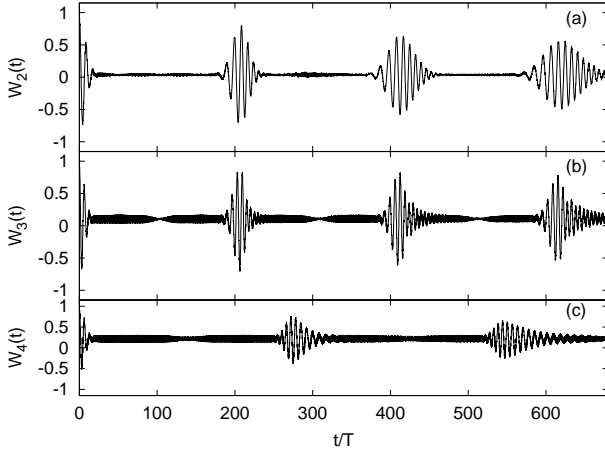


FIG. 4: Collapse and revival of the multiphoton Rabi oscillations. Three-level system population inversion is shown with the field initially in a coherent state. (a) Two-photon resonance with coupling parameters $\lambda/\omega = 0.02$, $\mu/\omega = 0.1$ and mean photon number $\bar{N} = 20$. (b) Three-photon resonance with parameters $\lambda/\omega = 0.02$, $\mu/\omega = 0.2$ and mean photon number $\bar{N} = 30$. (c) Same as (b) but for four-photon resonance and $\bar{N} = 50$.

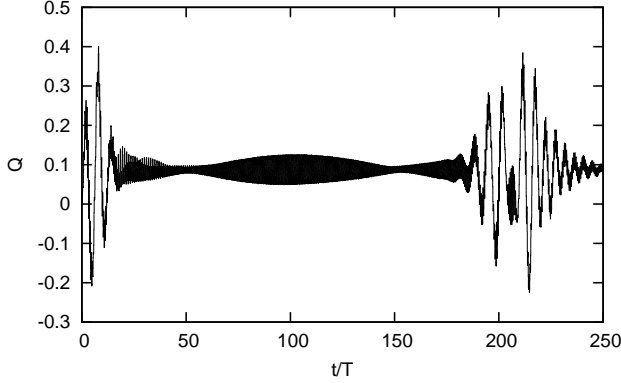


FIG. 5: Mandel's Q -factor versus scaled time for the setup of Fig. 4(b).

is seen from this figure during the collapse and revival of the multiphoton Rabi oscillations photons' antibunching ($Q < 0$) takes place.

Concluding, we see that the numerical simulations are in agreement with analytical treatment in the multiphoton resonant approximation and confirm the revealed physical picture described above.

IV. DEEP STRONG COUPLING REGIME

In this section we present results of numerical calculations that demonstrate the properties of the system in the deep strong coupling regime. In particular, we perform calculations for the ground state of the system.

The results obtained in the previous section rely on a resonant approximation, which is valid for not too strong coupling (26). However, for certain experimental conditions, interaction strengths can reach deep strong coupling regime. For those couplings, the application of a resonant approximation is not justified anymore. Hence, one needs new methods to examine the system in this parameter range. The Hamiltonian may be written in matrix form in the basis $|g_1, N\rangle$, $|g_2, N\rangle$, and $|e, N\rangle$ (where $N = 0, 1, 2, \dots$), which is the eigenbasis of the noninteracting Hamiltonian with $\Delta = 0$:

$$\hat{H} = \begin{bmatrix} \varepsilon_g + \frac{\hbar\omega}{2} & \Delta & 0 & -\hbar\mu & 0 & \hbar\lambda & 0 & 0 & 0 & \dots \\ \Delta & \varepsilon_g + \frac{\hbar\omega}{2} & 0 & 0 & \hbar\mu & -\hbar\lambda & 0 & 0 & 0 & \dots \\ 0 & 0 & \varepsilon_e + \frac{\hbar\omega}{2} & \hbar\lambda & -\hbar\lambda & 0 & 0 & 0 & 0 & \dots \\ -\hbar\mu & 0 & \hbar\lambda & \varepsilon_g + \frac{3\hbar\omega}{2} & \Delta & 0 & -\sqrt{2}\hbar\mu & 0 & \sqrt{2}\hbar\lambda & \dots \\ 0 & \hbar\mu & -\hbar\lambda & \Delta & \varepsilon_g + \frac{3\hbar\omega}{2} & 0 & 0 & \sqrt{2}\hbar\mu & -\sqrt{2}\hbar\lambda & \dots \\ \hbar\lambda & -\hbar\lambda & 0 & 0 & 0 & \varepsilon_e + \frac{3\hbar\omega}{2} & \sqrt{2}\hbar\lambda & -\sqrt{2}\hbar\lambda & 0 & \dots \\ 0 & 0 & 0 & -\sqrt{2}\hbar\mu & 0 & \sqrt{2}\hbar\mu & \varepsilon_g + \frac{5\hbar\omega}{2} & \Delta & 0 & \dots \\ 0 & 0 & 0 & 0 & \sqrt{2}\hbar\mu & -\sqrt{2}\hbar\lambda & \Delta & \varepsilon_g + \frac{5\hbar\omega}{2} & 0 & \dots \\ 0 & 0 & 0 & \sqrt{2}\hbar\lambda & -\sqrt{2}\hbar\lambda & 0 & 0 & 0 & \varepsilon_e + \frac{5\hbar\omega}{2} & \dots \\ \vdots & \vdots & \vdots & \vdots & \vdots & \vdots & \vdots & \vdots & \vdots & \ddots \end{bmatrix}, \quad (40)$$

where the order of the columns and rows is $|g_1, 0\rangle$, $|g_2, 0\rangle$, $|e, 0\rangle$, $|g_1, 1\rangle$, $|g_2, 1\rangle$, $|e, 1\rangle, \dots$. The Hamiltonian repre-

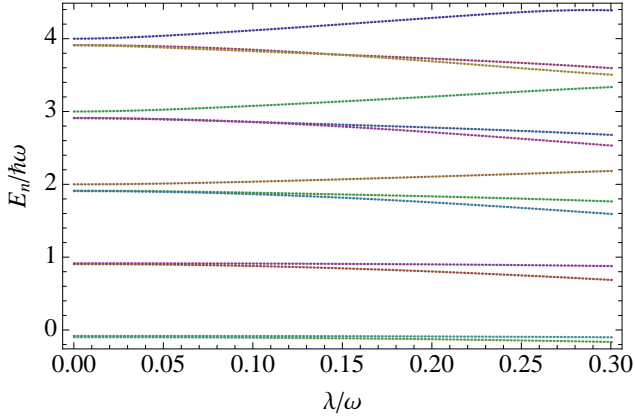


FIG. 6: (Color online) Lowest thirteen energy levels at the two-photon resonance: $\omega_0 = 2\omega$. The scaled energy $E_n/\hbar\omega$ is plotted as a function of the scaled coupling strength λ/ω at $\mu/\omega = 0.3$ and $\Delta/\hbar\omega = 0.01$. The energy is counted from $\varepsilon_g + \hbar\omega/2$.

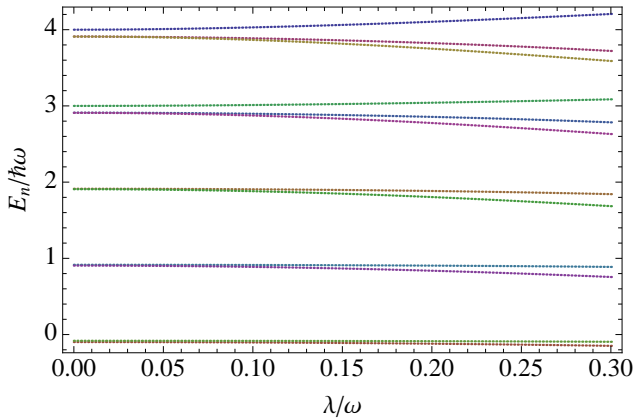


FIG. 7: (Color online) Lowest twelve energy levels at the three-photon resonance: $\omega_0 = 3\omega$. The scaled energy $E_n/\hbar\omega$ is plotted as a function of the scaled coupling strength λ/ω at $\mu/\omega = 0.3$ and $\Delta/\hbar\omega = 0.01$.

sents a block tridiagonal matrix for which there are effective algorithms for diagonalization. Using the Arnoldi algorithm [27] we have diagonalized the Hamiltonian (40). For these calculations the energy is counted from $\varepsilon_g + \hbar\omega/2$. In Figs. 6 and 7 we plot energy levels as a function of the scaled coupling strength λ/ω at the two- and three-photon resonances for the moderately strong coupling $\mu/\omega = 0.3$. As is seen starting from the level $n = \omega_0/\omega$ threefold degenerated states are splitted and splitting energy increases for the large coupling strength in accordance with resonant approximation.

While in the JC model the ground state of the atom-photonic field system consists of a product of the atom's ground state and the photonic field's vacuum state, an inclusion of the terms $\sim \mu$ leads to a vacuum state (12)

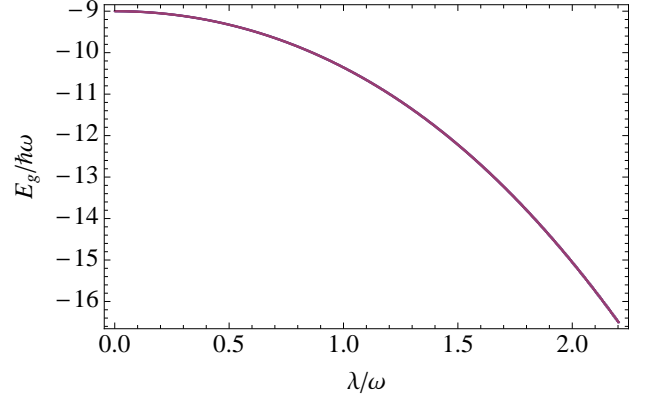


FIG. 8: The ground state scaled energy versus scaled coupling strength λ/ω at $\mu/\omega = 3$ and $\omega_0/\omega = 10$.

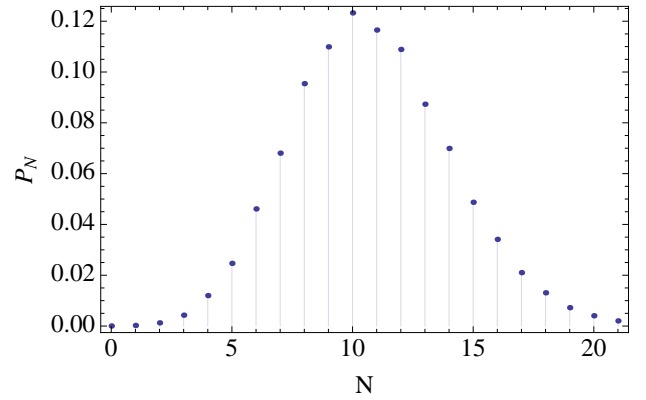


FIG. 9: Photon number probability distribution P_N as a function of photon number in the ground state at $\omega_0/\omega = 10$, $\mu/\omega = 3$, and $\lambda/\omega = 1$.

containing photons in the coherent states. With the large coupling λ one can expect qutrit-photonic field entangled ground state containing large number of photons in the coherent states. The number of photons will depend on both coupling parameters μ and λ . In Fig. 8 it is plotted the ground state energy versus scaled coupling strength λ/ω for large μ and ω_0 (henceforth we set $\Delta/\hbar\omega = 0.1$). In Figs. 9 and 10 we show photon number probability distribution P_N in the ground state at $\lambda/\omega = 1$ and $\lambda/\omega = 2$, respectively. As is seen from this figures the mean number of photons in the ground state is quite large and strongly depends on the coupling λ between qutrit excited and ground states. For both setups Mandel's Q -factor (39) is calculated to be $Q \simeq 10^{-2}$, which means that for large μ and λ photons exhibit the Poissonian statistics.

In order to obtain optimal conditions for the qutrit-oscillator entangled states, we now analyze the entanglement properties in the ground state. Various measures of entanglement exist. One commonly used entanglement

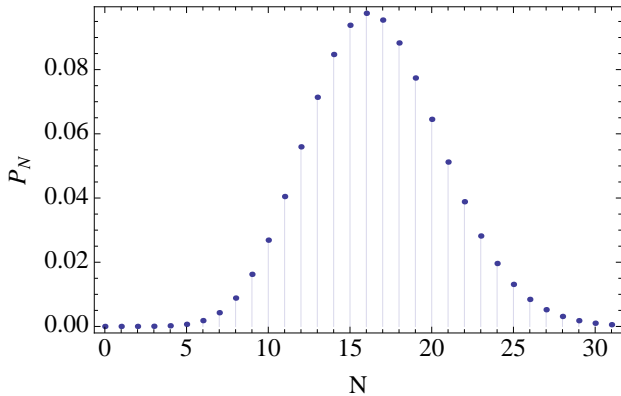


FIG. 10: Same as Fig. 9 but for $\lambda/\omega = 2$.

measures for pure states is the von Neumann entropy. The latter for the qutrit will be defined as:

$$S_3 = -\text{Tr} [\rho_r \log_3 \rho_r], \quad (41)$$

where

$$\rho_r = \text{Tr}_{\text{photon}} [|\Psi\rangle\langle\Psi|] \quad (42)$$

is the qutrit reduced density matrix and $|\Psi\rangle$ is the wave function of qutrit-photon field combined system. The von Neumann entropy satisfies the inequality $0 \leq S_3 \leq 1$, where the lower bound is reached if and only if $|\Psi\rangle$ is a product state, while upper bound is reached if and only if $|\Psi\rangle$ is a maximally entangled state. Thus, rising from the Hamiltonian (40) we calculate the ground state eigenvector of the combined system and then evaluate the entropy of that state according to Eqs. (42) and (41). In Figs. 11 and 12 the qutrit's entropy S_3 , which quantifies the qutrit-photon field entanglement in the ground state, is displayed as a function of coupling parameters. Figure 11 is plotted for the fixed μ , while Fig. 12 for the fixed λ . As is seen from last two figures, there are optimal values for the maximal entanglement and for very large couplings the latter vanishes.

V. CONCLUSION

We have presented a theoretical treatment of the quantum dynamics of a qutrit in a polar- Λ configuration interacting with a single-mode photonic field in the ultra-strong and deep strong coupling regimes. For the ultra-strong couplings we have solved the Schrödinger equation in the multiphoton resonant approximation and obtained simple analytical expressions for the eigenstates and eigenenergies. In this case for the n -photon resonance we have entangled states of a qutrit and position-displaced Fock states. We have also investigated the temporal quantum dynamics of the considered system at the multiphoton resonance and showed that due to the mean

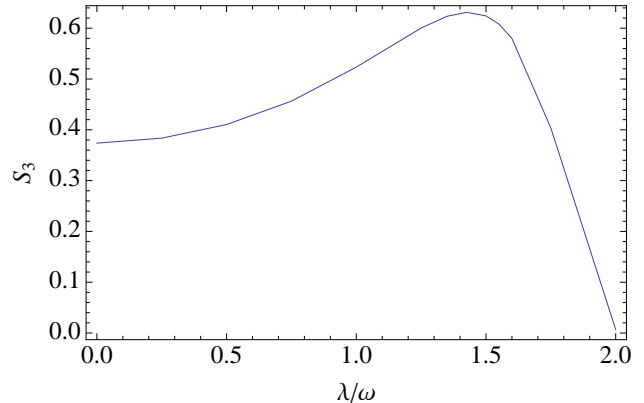


FIG. 11: The qutrit's entropy S_3 in the ground state as a function of λ/ω at $\omega_0/\omega = 10$ and $\mu/\omega = 3$.

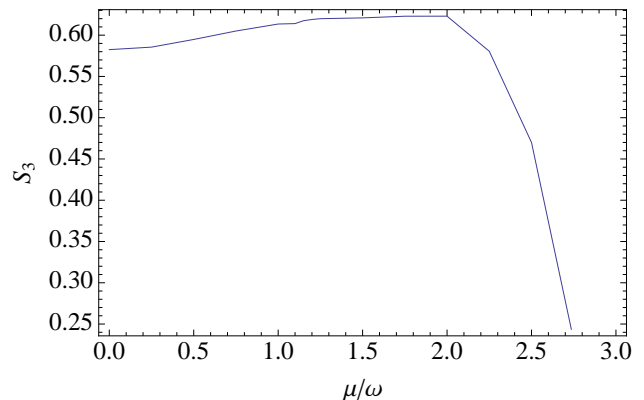


FIG. 12: The qutrit's entropy S_3 in the ground state as a function of μ/ω at $\omega_0/\omega = 10$ and $\lambda/\omega = 2$.

dipole moments in the lower states it is possible Rabi oscillations of population inversion with periodic multiphoton exchange between a qutrit and a photonic field. For the quantized field prepared initially in a coherent state multiphoton Rabi oscillations collapse/revive and photons' antibunching takes place. In the deep strong coupling regime particular emphasis is placed on the ground state of the system. The latter exhibits strictly nonclassical properties. In particular, it has been shown that for the large coupling parameters μ and λ we have qutrit-photon field entangled ground state containing large number of photons in the coherent states. The proposed model may have diverse applications in QED with artificial atoms, especially in the circuit QED, where the considered qutrit configuration and deep strong coupling regime are foreseen.

Acknowledgments

This work was supported by State Committee of Science of Republic of Armenia, Project No. 13RF-002 and Russian Foundation for Basic Research, Project No. 13-02-90600.

Appendix A: Equivalence of polar- Λ and L configurations

In this Appendix we prove equivalence of polar- Λ and L configurations. As an illustrative physical system we consider an electron in a symmetric 1D double well potential. In this case the selection rule for optical transitions is: the matrix element of the electric dipole moment is nonzero for the states of different parity. Consider the case when the first two eigenstates are localized in the wells of the potential, while the higher eigenstate is delocalized. This situation can also be realized for flux qubits [22]. Thus, the ground eigenstate is an even function, the eigenstate corresponding to adjacent level is an odd function, and finally, the eigenstate of the excited state is an even function. According to selection rule we have L configuration and in the single mode photonic field one can write the Hamiltonian:

$$\hat{H}_{L+ph} = \hbar\omega \left(\hat{a}^+ \hat{a} + \frac{1}{2} \right) + \hat{H}_L$$

$$+ \epsilon d_{g_1 g_2} \hat{S}_{g_1 \leftrightarrow g_2} (\hat{a}^+ + \hat{a}) + \epsilon d_{g_2 e} \hat{S}_{g_2 \leftrightarrow e} (\hat{a}^+ + \hat{a}), \quad (A1)$$

where

$$\hat{H}_L = \begin{pmatrix} \varepsilon_{g_1} & 0 & 0 \\ 0 & \varepsilon_{g_2} & 0 \\ 0 & 0 & \varepsilon_e \end{pmatrix}, \quad (A2)$$

$d_{g_1 g_2}$, $d_{g_2 e}$ are transition dipole moments, $\epsilon(\hat{a}^+ + \hat{a})$ is the electric field operator, and

$$\hat{S}_{g_1 \leftrightarrow g_2} = \begin{pmatrix} 0 & 1 & 0 \\ 1 & 0 & 0 \\ 0 & 0 & 0 \end{pmatrix}, \hat{S}_{g_2 \leftrightarrow e} = \begin{pmatrix} 0 & 0 & 0 \\ 0 & 0 & 1 \\ 0 & 1 & 0 \end{pmatrix} \quad (A3)$$

are transition operators. Now let us apply unitary transformation ($\hat{U}\hat{L}\hat{U}^+$) defined as:

$$\hat{U} = \frac{1}{\sqrt{2}} \begin{pmatrix} 1 & -1 & 0 \\ 1 & 1 & 0 \\ 0 & 0 & \sqrt{2} \end{pmatrix}. \quad (A4)$$

For the transformed operators we obtain:

$$\hat{H}'_L = \begin{pmatrix} \frac{\varepsilon_{g_1} + \varepsilon_{g_2}}{2} & \frac{\varepsilon_{g_1} - \varepsilon_{g_2}}{2} & 0 \\ \frac{\varepsilon_{g_1} - \varepsilon_{g_2}}{2} & \frac{\varepsilon_{g_1} + \varepsilon_{g_2}}{2} & 0 \\ 0 & 0 & \varepsilon_e \end{pmatrix}, \quad (A5)$$

$$\hat{S}'_{g_1 \leftrightarrow g_2} = \begin{pmatrix} -1 & 0 & 0 \\ 0 & 1 & 0 \\ 0 & 0 & 0 \end{pmatrix} \equiv \hat{S}_L, \quad (A6)$$

$$\hat{S}'_{g_2 \leftrightarrow e} = -\frac{1}{\sqrt{2}} \begin{pmatrix} 0 & 0 & 1 \\ 0 & 0 & -1 \\ 1 & -1 & 0 \end{pmatrix} \equiv -\frac{1}{\sqrt{2}} \hat{S}_t. \quad (A7)$$

Now it is easy to see that the transformed Hamiltonian corresponds to polar- Λ configuration considered in the paper (see Eq. (2)) with the parameters:

$$\begin{aligned} \varepsilon_g &= \frac{\varepsilon_{g_1} + \varepsilon_{g_2}}{2}; \quad \Delta = \frac{\varepsilon_{g_1} - \varepsilon_{g_2}}{2}; \\ \mu &= \frac{\epsilon d_{g_1 g_2}}{\hbar}; \quad \lambda = -\frac{1}{\sqrt{2}} \frac{\epsilon d_{g_2 e}}{\hbar}. \end{aligned} \quad (A8)$$

The terms \hat{S}_L and \hat{S}_t describe electric-dipole moment matrix elements. So, the diagonal elements are the mean dipole moments and are described by the terms proportional to \hat{S}_L . This is also obvious in the coordinate picture. In the symmetric double well where the probability of tunnel transition between the "left" and "right" potential wells is small ($|\Delta| \ll \varepsilon_g$), we have nearly degenerated ground state and can use two equivalent bases. In a L configuration the two lowest energy eigenstates are of the form $|\pm\rangle = (|\text{left}\rangle \pm |\text{right}\rangle)/\sqrt{2}$, where $|\text{left}\rangle$ and $|\text{right}\rangle$ are the basis wave functions in the polar- Λ configuration and represent the situations that the particle is in the left or right potential well with opposite mean dipole moments.

-
- [1] B. W. Shore, P. L. Knight, *Journal of Modern Optics* **40**, 1195 (1993).
 [2] J. M. Raimond, M. Brune, S. Haroche, *Rev. Mod. Phys.* **73**, 565 (2001).

- [3] E. T. Jaynes, F. W. Cummings, *Proc. IEEE* **51**, 89 (1963).
 [4] L. Mandel and E. Wolf, *Optical Coherence and Quantum Optics* (Cambridge University Press, Cambridge 1995).

- [5] M. O. Scully, M. S. Zubairy, *Quantum Optics* (Cambridge University Press, Cambridge 1997).
- [6] M. A. Nielsen, I. L. Chuang, *Quantum computation and quantum information* (Cambridge University Press, Cambridge 2010).
- [7] E. Peter *et al.*, Phys. Rev. Lett. **95**, 067401 (2005); K. Hennessy *et al.*, Nature **445**, 896 (2007).
- [8] A. Wallraff *et al.*, Nature **431**, 162 (2004).
- [9] O. V. Kibis, Phys. Rev. B **81**, 165433 (2010).
- [10] D. Bruß and C. Macchiavello, Phys. Rev. Lett. **88**, 127901 (2002); N. K. Langford, R. B. Dalton, M. D. Harvey, J. L. O'Brien, G. J. Pryde, A. Gilchrist, S. D. Bartlett, A. G. White, Phys. Rev. Lett. **93**, 053601 (2004).
- [11] H. K. Avetissian, G. F. Mkrtchian, Phys. Rev. A **66**, 033403 (2002).
- [12] H. K. Avetissian, B. R. Avchyan, G. F. Mkrtchian, Phys. Rev. A **74**, 063413 (2006).
- [13] L. D. Landau and E. M. Lifshitz, *Quantum mechanics: non relativistic theory*, (Pergamon Press, Oxford, U.K., 1965).
- [14] T. Niemczyk *et al.*, Nature Physics **6**, 772 (2010).
- [15] P. Goy, J. M. Raimond, M. Gross, and S. Haroche, Phys. Rev. Lett. **50**, 1903 (1983).
- [16] H. Walther, B. T. H. Varcoe, B. G. Englert, and T. Becker, Rep. Prog. Phys. **69**, 1325 (2006).
- [17] C. Ciuti, G. Bastard and I. Carusotto, Phys. Rev. B **72**, 115303 (2005). G. Gunter *et al.*, Nature (London) **458**, 178 (2009); G. Scalari *et al.*, Science **335**, 1323 (2012).
- [18] D. Ballester, G. Romero, J.J. Garcia-Ripoll, F. Deppe, E. Solano, Phys. Rev. X **2**, 021007 (2012); G. Romero, D. Ballester, Y. M. Wang, V. Scarani, E. Solano, Phys. Rev. Lett. **108**, 120501 (2012); Shu He *et al.*, Phys. Rev. A **86**, 033837 (2012).
- [19] H. K. Avetissian, G. F. Mkrtchian, Phys. Rev. A **88**, 043811 (2013).
- [20] J. Casanova, G. Romero, I. Lizuain, J. J. Garcia-Ripoll, and E. Solano, Phys. Rev. Lett. **105**, 263603 (2010); S. Ashhab and F. Nori, Phys. Rev. A **81**, 042311 (2010); D. Hagenmüller, S. De Liberato and C. Ciuti, Phys. Rev. B **81**, 235303 (2010); S. De Liberato, Phys. Rev. Lett. **112**, 016401 (2014).
- [21] Y.-x. Liu, J. Q. You, L. F. Wei, C. P. Sun, and F. Nori, Phys. Rev. Lett. **95**, 087001 (2005).
- [22] J. Bourassa, J. M. Gambetta, A. A. Abdumalikov Jr, O. Astafiev, Y. Nakamura, and A. Blais, Phys. Rev. A **80**, 032109 (2009).
- [23] A. J. Leggett, S. Chakravarty, A. T. Dorsey, M. P. A. Fisher, A. Garg, and W. Zwerger, Rev. Mod. Phys. **59**, 1 (1987).
- [24] R. Rouse, S. Han, and J. E. Lukens, Phys. Rev. Lett. **75**, 1614 (1995); J. R. Friedman, V. Patel, W. Chen, S. K. Tolpygo, J. E. Lukens, Nature **406**, 43 (2000).
- [25] J. E. Mooij, T. P. Orlando, L. Levitov, Lin Tian, Caspar H. van der Wal, and Seth Lloyd, Science **285**, 1036 (1999); T. P. Orlando, J. E. Mooij, Lin Tian, Caspar H. van der Wal, L. S. Levitov, Seth Lloyd, and J. J. Mazo, Phys. Rev. B **60**, 15398 (1999).
- [26] W. H. Press, S. A. Teukolsky, W. T. Vetterling, B. P. Flannery, *Numerical Recipes in C* (Cambridge University Press, Cambridge, 1992).
- [27] Wolfram Research, Inc., *Mathematica, Version 9.0* (Champaign, IL 2012).